PERGAMON

International Journal of Solids and Structures 40 (2003) 1109–1137

INTERNATIONAL JOURNAL OF SOLIDS and STRUCTURES

www.elsevier.com/locate/ijsolstr

Application of theorem of minimum potential energy to a complex structure Part II: three-dimensional analysis

Eric C. Preissner *, Jack R. Vinson

Department of Mechanical Engineering, University of Delaware, Newark, DE 19716, USA

Received 7 June 2002; received in revised form 18 October 2002

Abstract

A cylindrical shell with a non-circular cross-section consisting of flat sides and circular arc corners is analyzed using the theorem of minimum potential energy. The three-dimensional analysis builds on previous two-dimensional work. The potential energy expression for the structure is developed, including first-order transverse shear deformation effects. All unknown displacements are represented by power series, and the potential energy expression is rewritten in terms of the summation convention for the power series. The variation of the potential energy expression is taken, leading to a linear system of equations that is solved for the unknown power series coefficients. With the displacements determined, stresses are calculated for a composite sandwich construction. An examination of both short shells (less than twice the boundary layer length) and long shells (more than twice the boundary layer length) is made. The MPE method with power series is found to predict behavior well for short shells, but not for long shells.

Keywords: Minimum potential energy; Non-circular cylinder; Quadratic programming; Power series

1. Introduction

Reported herein is the investigation of three-dimensional cylindrical shells with non-circular cross-sections subjected to constant internal pressure (see Figs. 1 and 2). Both short and long shells (with respect to bending boundary layer length) are examined, and due to lack of experimental data, the results are compared to a finite element analysis. The work for the three-dimensional case builds on the two-dimensional analysis described previously in Part I (Preissner and Vinson, 2002a). Part I of this work also gives a summary of the previous research performed in the areas of the application of the MPE method to shell structures and the analysis of non-circular cylindrical shells.

* Corresponding author. Address: 1925 Timber Trail, Ann Arbor, MI 48103-2395, USA. Tel.: +1-734-769-1055.
E-mail address: epreissner@hotmail.com (E.C. Preissner).

0020-7683/02/$ - see front matter
PII: S0020-7683(02)00655-8

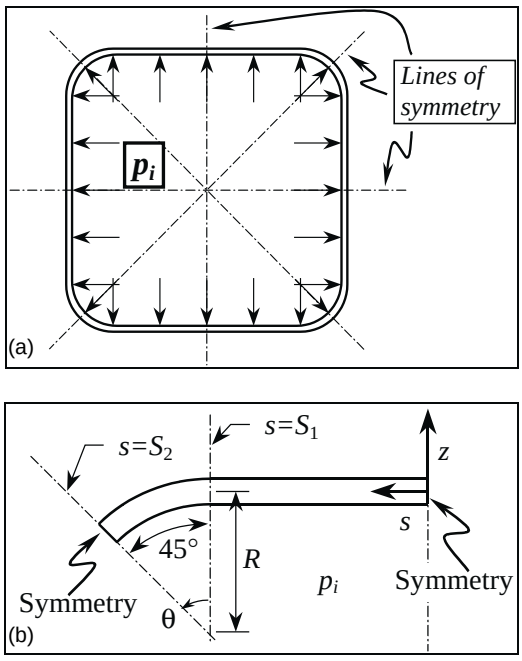

Fig. 1. (a) Full non-circular cross-section shape. (b) Details of the geometry.

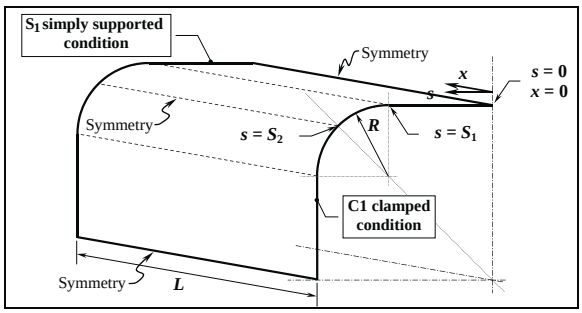

Fig. 2. Representation of shell mid-plane for three-dimensional problem.

2. Formulation

The motivation behind using the MPE method was to find practical, approximate (yet accurate) solutions to (ultimately) the three-dimensional problem. Previous two-dimensional solution methods were too complicated to readily extend to three dimensions. Using the current formulation, the two-dimensional problem was solved first as a building block toward the three-dimensional solution, and was checked against the Forbes solution (Forbes, 1999) and finite element analyses (see Part I).

The elimination method (Greenberg, 1998) is appropriate for simple problems. For more complicated problems such as the two-dimensional analysis of Part I, constrained minimization via Lagrange multipliers was successfully applied (Preissner and Vinson, 2002a). With the added complexity of a three-dimensional

analysis, the Lagrange multiplier method failed to solve the problem, and the more advanced technique of quadratic programming was employed.

Quadratic programming is a technique of optimization used when the objective function (the function to be extremized; the PE expression in the current case) is of quadratic form, and the equality (or inequality) constraints are linear. While more robust of a method than either elimination or simple constrained optimization, this came at a complexity that forced the use of a pre-written IMSL FORTRAN solution routine (Anonymous, 1994). Formally, this is the solution to problems of the form:

$$\min_{\mathbf{x}\in R^n} \ \mathbf{g}^{\mathrm{T}}\mathbf{x} + \frac{1}{2}\mathbf{x}^{\mathrm{T}}\mathbf{H}\mathbf{x} \tag{1}$$

subject to the constraints:

$$\begin{aligned} \mathbf{A}_1\mathbf{x} &= \mathbf{b}_1 \\ \mathbf{A}_2\mathbf{x} &\geqslant \mathbf{b}_2 \end{aligned} \tag{2}$$

The vectors $\mathbf{b}_1$, $\mathbf{b}_2$, and $\mathbf{g}$ and the matrices $\mathbf{H}$, $\mathbf{A}_1$, and $\mathbf{A}_2$ are known. The routine used is DQPROG, and is based on Powell's implementation of the Goldfarb and Idnani dual quadratic programming algorithm for convex quadratic programming problems of the form above (see Goldfarb and Idnani, 1983; Powell, 1983, 1985). Additional general and rigorous discussion of this method and its variations can be found in Gill and Murray (1974) and Fletcher (1981).

In this method, the PE expression is developed as before. Next, the linear terms in the PE expression are identified (vector $\mathbf{g}$ in Eq. (1)), and the Hessian for the PE expression is developed (matrix $\mathbf{H}$ in Eq. (1)). The Hessian is defined as:

$$H_{ij} = \frac{\partial^2 V}{\partial p_i \partial p_j} \tag{3}$$

Thus, the Hessian is a matrix whose coefficients are defined as the second derivatives of the PE function with respect to each of the variables in the expression. In addition to this, the coefficients for the linear constraints are developed and placed in the matrix $\mathbf{A}_1$. All of the constraints in this problem are equality constraints, so there is no matrix $\mathbf{A}_2$.

Due to the complexity of the expressions and the desire to have a method that was general enough to handle various displacement trial functions, the filling of the necessary vectors and matrices was written as a FORTRAN program. Once the inputs were generated, they were passed to the IMSL DQPROG routine. The output of DQPROG is not only a vector with the solution (the trial function coefficients), but also includes a vector of constraints that were active in (i.e., influenced) the solution, and a vector containing the Lagrange multiplier estimates for the final active constraints. The benefits of this formulation are that it is slightly more concise than the previous constrained optimization and, most importantly, was able to find solutions where the other methods failed. The drawback to the approach is that it is a "black box," relying on a supplied solution technique. In that respect, when the method fails, there is little adjustment that can be made and other techniques must be sought.

3. Geometry and loads

This paper examines a cylinder defined using the same rounded square cross-section as was analyzed in Part I (see Figs. 1 and 2 and Preissner and Vinson, 2002a). Again, the use of the modified square section allows for the maximum use of symmetry (Fig. 1(b)). The composition of the structure is assumed to be a

composite laminate, and more specifically a composite sandwich. The three-dimensional MPE analysis includes transverse shear deformation effects but neglects transverse normal stress. Structural coupling (the inclusion of $(\ )_{16}$, $(\ )_{26}$, A_{45}, or B_{ij} terms) is *not* included.

Due to the symmetry, the full square section is reduced to a one-eighth section for analysis. No symmetry can be applied in the axial direction for this case. The coordinate system is a right-handed x–s–z system, with the x-direction along the axis of the cylinder, the s-direction around the circumference from the top, and the z-direction through the thickness. The cylinder extends in the positive x-direction, and is of length L. The extent of the initial flat section is from $s = 0$ to $s = S_1$. The overall extent of the one-eighth section is $s = S_2$, so that the extent of the circular arc corner is $s = (S_2 - S_1)$. The radius of the corner is designated R, and the constant internal pressure is p_i.

Because the structure is composed of straight sections connected by circular arcs, the formulation of the governing equations is different in those sections. *Definitions* of strains, stresses, and potential energy expressions are not common across the junction between the flat and curved section at $s = S_1$. All physical quantities (e.g., u, v, w, N, M, σ, etc.) must be, of course, continuous across this junction. Symmetry boundary conditions are imposed at the $s = 0$, $s = S_2$ edges, while matching conditions are imposed at the junction where $s = S_1$. The $x = 0$ edge utilizes the C1 clamped boundary condition, while the $x = L$ edge utilizes the S1 simply supported boundary condition. The specifics of these boundary conditions will be given in the subsequent section.

4. Strain–displacement relations and boundary conditions

The assumed strain–displacement relations for a flat plate are (neglecting second-order terms; see Vinson, 1999 or Ochoa and Reddy, 1992):

$$\varepsilon_x = \frac{\partial u_0}{\partial x} + z\frac{\partial \bar{\beta}_x}{\partial x} = \varepsilon_{x_0} + z\kappa_x \qquad \varepsilon_y = \frac{\partial v_0}{\partial y} + z\frac{\partial \bar{\beta}_y}{\partial y} = \varepsilon_{y_0} + z\kappa_y \qquad \varepsilon_z = 0 \tag{4a}$$

$$\varepsilon_{xz} = \frac{1}{2}\left(\bar{\beta}_x + \frac{\partial w}{\partial x}\right) \qquad \varepsilon_{yz} = \frac{1}{2}\left(\bar{\beta}_y + \frac{\partial w}{\partial y}\right) \tag{4b}$$

$$\varepsilon_{xy} = \frac{1}{2}\left(\frac{\partial u_0}{\partial y} + \frac{\partial v_0}{\partial x}\right) + \frac{z}{2}\left(\frac{\partial \bar{\beta}_x}{\partial y} + \frac{\partial \bar{\beta}_y}{\partial x}\right) \tag{4c}$$

The strain–displacement relations for a circular shell of radius R are given as (with the s-direction along the shell, noting that $\partial s = R\partial\theta$; see Vinson, 1993, Eqs. (15.2), (15.5) and (15.8)):

$$\varepsilon_x = \frac{\partial u_0}{\partial x} + z\frac{\partial \bar{\beta}_x}{\partial x} = \varepsilon_{x_0} + z\kappa_x \qquad \varepsilon_\theta = \left(\frac{\partial v_0}{\partial s} + \frac{w}{R}\right) + z\frac{\partial \bar{\beta}_\theta}{\partial s} = \varepsilon_{\theta_0} + z\kappa_\theta \qquad \varepsilon_z = 0 \tag{5a}$$

$$\varepsilon_{x\theta_0} = \frac{1}{2}\left(\frac{\partial v_0}{\partial x} + \frac{\partial u_0}{\partial s}\right) \qquad \varepsilon_{xz} = \frac{1}{2}\left(\bar{\beta}_x + \frac{\partial w}{\partial x}\right) \qquad \varepsilon_{\theta z} = \frac{1}{2}\left(\bar{\beta}_\theta + \frac{\partial w}{\partial s} - \frac{v_0}{R}\right) \tag{5b}$$

The forms of the trial displacement functions are taken to be the following finite-ordered, two-dimensional power series:

$$
\begin{aligned}
w_1(s,x) &= \sum_{i=0}^{M}\sum_{j=0}^{N} a_{i,j}s^i x^j \qquad & w_2(s,x) &= \sum_{i=0}^{M}\sum_{j=0}^{N} b_{i,j}s^i x^j \\
v_1(s,x) &= \sum_{i=0}^{M}\sum_{j=0}^{N} c_{i,j}s^i x^j \qquad & v_2(s,x) &= \sum_{i=0}^{M}\sum_{j=0}^{N} d_{i,j}s^i x^j \\
u_1(s,x) &= \sum_{i=0}^{M}\sum_{j=0}^{N} f_{i,j}s^i x^j \qquad & u_2(s,x) &= \sum_{i=0}^{M}\sum_{j=0}^{N} g_{i,j}s^i x^j \\
\bar{\beta}_{s_1}(s,x) &= \sum_{i=0}^{M}\sum_{j=0}^{N} k_{i,j}s^i x^j \qquad & \bar{\beta}_{s_2}(s,x) &= \sum_{i=0}^{M}\sum_{j=0}^{N} l_{i,j}s^i x^j \\
\bar{\beta}_{x_1}(s,x) &= \sum_{i=0}^{M}\sum_{j=0}^{N} p_{i,j}s^i x^j \qquad & \bar{\beta}_{x_2}(s,x) &= \sum_{i=0}^{M}\sum_{j=0}^{N} q_{i,j}s^i x^j
\end{aligned}
\tag{6}
$$

Using different limits on the s and x summations allows different orders of expansions in those directions, if desired. Note that the comma separating the i and j subscripts in Eq. (6) is only for clarity and does not represent differentiation. The total number of unknown expansion coefficients will therefore be $10(M+1)(N+1)$.

The boundary conditions are as follows. At $s = 0$ the zero-shear symmetry condition is used, as in the two-dimensional analysis:

$$
\begin{aligned}
&1.\ v_1(0,x) = 0 \\
&2.\ Q_s(0,x) = 0 \\
&3.\ \bar{\beta}_{s_1}(0,x) = 0
\end{aligned}
\tag{7}
$$

Matching conditions are established at $s = S_1$, notably more extensive than those for the two-dimensional case. These boundary conditions are separated into two groups. As these boundary conditions are being specified on an $s =$ constant edge, the first set consists of boundary conditions that address quantities normally specified on such edges. These are:

$$
\begin{aligned}
&4.\ w_1(S_1,x) = w_2(S_1,x) \\
&5.\ v_1(S_1,x) = v_2(S_1,x) \\
&6.\ u_1(S_1,x) = u_2(S_1,x) \\
&7.\ \bar{\beta}_{s_1}(S_1,x) = \bar{\beta}_{s_2}(S_1,x) \\
&8.\ [N_s(S_1,x)]_1 = [N_s(S_1,x)]_2 \\
&9.\ [N_{xs}(S_1,x)]_1 = [N_{xs}(S_1,x)]_2 \\
&10.\ [M_s(S_1,x)]_1 = [M_s(S_1,x)]_2 \\
&11.\ [M_{xs}(S_1,x)]_1 = [M_{xs}(S_1,x)]_2 \\
&12.\ [Q_s(S_1,x)]_1 = [Q_s(S_1,x)]_2
\end{aligned}
\tag{8}
$$

The second set consists of those boundary conditions that address quantities that are not normally specified on $s =$ constant edges. Yet, through engineering reasoning, these quantities should remain continuous in the circumferential direction. These are:

$$
\begin{aligned}
&13.\ \bar{\beta}_{x_1}(S_1,x) = \bar{\beta}_{x_2}(S_1,x)\\
&14.\ [N_x(S_1,x)]_1 = [N_x(S_1,x)]_2\\
&15.\ [M_x(S_1,x)]_1 = [M_x(S_1,x)]_2\\
&16.\ [Q_x(S_1,x)]_1 = [Q_x(S_1,x)]_2
\end{aligned}
\tag{9}
$$

At $s = S_2$ there are the same three symmetry conditions as at $s = 0$:

$$
\begin{aligned}
&17.\ v_2(S_2,x) = 0\\
&18.\ Q_s(S_2,x) = 0\\
&19.\ \bar{\beta}_{s_2}(S_2,x) = 0
\end{aligned}
\tag{10}
$$

There are now also boundary conditions in the x-direction. Using a C1 clamped condition (i.e., maintaining zero lateral and in-plane deflections, zero rotation, and zero in-plane shear resultant; the C2 condition exchanges zero in-plane deflection for zero in-plane normal resultant; see Vinson, 1999, Eq. (3.51)), the boundary conditions at $x = 0$ are:

$$
\begin{aligned}
&20.\ w_1(s,0) = 0\\
&21.\ w_2(s,0) = 0\\
&22.\ \bar{\beta}_{x_1}(s,0) = 0\\
&23.\ \bar{\beta}_{x_2}(s,0) = 0\\
&24.\ u_1(s,0) = 0\\
&25.\ u_2(s,0) = 0\\
&26.\ N_{xs_1}(s,0) = 0\\
&27.\ N_{xs_2}(s,0) = 0
\end{aligned}
\tag{11}
$$

The authors see no way to restrict these boundary conditions on the flat and circular portions to only those portions (i.e., only w_1 over $0 \to S_1$ and w_2 over $S_1 \to S_2$). It is not clear that it is necessary to do so. Using the S1 simple support condition (i.e., maintaining zero lateral and in-plane deflections, zero moment parallel to the edge, and zero in-plane shear resultant; the S2 condition exchanges zero in-plane deflection for zero in-plane normal resultant; see Vinson, 1999, Eq. (3.50)), the boundary conditions at $x = L$ are:

$$
\begin{aligned}
&28.\ w_1(s,L) = 0\\
&29.\ w_2(s,L) = 0\\
&30.\ M_{x_1}(s,L) = 0\\
&31.\ M_{x_2}(s,L) = 0\\
&32.\ u_1(s,L) = 0\\
&33.\ u_2(s,L) = 0\\
&34.\ N_{xs_1}(s,L) = 0\\
&35.\ N_{xs_2}(s,L) = 0
\end{aligned}
\tag{12}
$$

For both the C1 and S1 boundary conditions, there is no direct specification on the circumferential deflection, v. However, v does appear in the evaluation of boundary conditions #26, 27, 34, and 35, due to the definition of N_{xs}.

5. Application of boundary conditions

The number of constraints can not be determined yet (it is not equal to the number of boundary conditions) because, as seen below, most of the above boundary conditions will generate more than one constraint (unlike the two-dimensional problem).

Applying boundary condition #1 gives that:

$$v_1(0,x) = \sum_{i=0}^{M}\sum_{j=0}^{N} c_{i,j}(0)^i x^j$$
$$= c_{0,0} + c_{0,1}x + c_{0,2}x^2 + \cdots + c_{1,0}(0) + c_{1,1}(0)x + \cdots + c_{2,0}(0)^2 + c_{2,1}(0)^2 x + \cdots = 0$$

where the term $(0)^0 \equiv 1$. This can also be expressed as:

$$v_1(0,x) = \sum_{j=0}^{N} c_{0,j}x^j = c_{0,0} + c_{0,1}x + c_{0,2}x^2 + \cdots = 0$$

This is now a polynomial only in x; it must be satisfied for *all* values of x. The only way this condition can be satisfied is if all of the coefficients of the polynomial are equal to zero. Therefore, the first boundary condition results in:

$$c_{0,j} = 0 \quad j = 0, 1, \ldots, N \tag{13}$$

This form gives $(N+1)$ equations that will be used as constraints on the potential energy expression. Note that in the quadratic programming method, there are no explicit Lagrange multipliers like there were in the constrained minimization used in the two-dimensional case. The constraints are incorporated in a different manner, such that estimates for Lagrange multipliers are an output of the IMSL solution subroutine.

Neglecting $(\ )_{45}$ coupling terms, boundary condition #2 gives:

$$Q_s|_{s=0} = 2(A_{45}\varepsilon_{xz} + A_{44}\varepsilon_{sz}) = A_{44}\left(\bar{\beta}_{s_1} + \frac{\partial w_1}{\partial s}\right)_{s=0} = 0 \tag{14}$$

Using Eq. (6) and noting that power series can be manipulated term-by-term (see Greenberg, 1998, p. 179, or Arfken, 1966, Section 5.7):

$$\frac{\partial w_1(s,x)}{\partial s} = \frac{\partial}{\partial s}\sum_{i=0}^{M}\sum_{j=0}^{N} a_{i,j}s^i x^j = \sum_{i=0}^{M}\sum_{j=0}^{N}\frac{\partial}{\partial s}(a_{i,j}s^i x^j) = \sum_{i=1}^{M}\sum_{j=0}^{N} i a_{i,j}s^{i-1}x^j \tag{15}$$

Thus:

$$Q_s|_{s=0} = \left(\sum_{i=0}^{M}\sum_{j=0}^{N} k_{i,j}s^i x^j + \sum_{i=1}^{M}\sum_{j=0}^{N} i a_{i,j}s^{i-1}x^j\right)_{s=0} = 0$$

where, by taking $0^{(0)} \equiv 1$ and $0^{(i\neq 0)} = 0$, we obtain:

$$\sum_{j=0}^{N} k_{0,j}x^j + \sum_{j=0}^{N} a_{1,j}x^j = 0 \quad k_{0,0} + k_{0,1}x + k_{0,2}x^2 + \cdots + a_{1,0} + a_{1,1}x + a_{1,2}x^2 + \cdots = 0$$

Collect like powers of x:

$$(k_{0,0}+a_{1,0})+(k_{0,1}+a_{1,1})x+(k_{0,2}+a_{1,2})x^2+\cdots=0 \quad \sum_{j=0}^{N}(k_{0,j}+a_{1,j})x^j=0 \tag{16}$$

Again, this is a polynomial in x and it must be satisfied for any arbitrary value of x. Thus, the results of this boundary condition are expressed as the $(N+1)$ constraint equations of:

$$k_{0,j}+a_{1,j}=0 \quad j=0,1,\ldots,N \tag{17}$$

Applying boundary condition #3 gives:

$$\bar{\beta}_{s_1}(0,x)=\left(\sum_{i=0}^{M}\sum_{j=0}^{N}k_{i,j}(0)^i x^j\right)_{s=0}=0 \tag{18}$$

Similar to boundary condition #1, this can be reduced to:

$$\sum_{j=0}^{N}k_{0,j}x^j=k_{0,0}+k_{0,1}x+k_{0,2}x^2+\cdots=0$$

With the same logic as in boundary condition #1, the third boundary condition results in the $(N+1)$ constraint equations:

$$k_{0,j}=0 \quad j=0,1,\ldots,N \tag{19}$$

It can be seen that the combination of boundary conditions #2 and #3 results in the $(N+1)$ equations:

$$a_{1,j}=0 \quad j=0,1,\ldots,N \tag{20}$$

which can be used as the constraints, instead of Eq. (17).

The conditions in Eqs. (20), (13) and (19) could be incorporated into the problem by changing the lower bound on the s summation of w_1, v_1 and $\bar{\beta}_{s_1}$ to be as follows:

$$w_1(s,x)=\sum_{j=0}^{N}a_{0,j}x^j+\sum_{i=2}^{M}\sum_{j=0}^{N}a_{i,j}s^i x^j \qquad v_1(s,x)=\sum_{i=1}^{M}\sum_{j=0}^{N}c_{i,j}s^i x^j \qquad \bar{\beta}_{s_1}(s,x)=\sum_{i=1}^{M}\sum_{j=0}^{N}k_{i,j}s^i x^j$$

However, the more consistent way is to include them as constraints. Doing it this way benefits the potential energy expression by keeping the indices more consistent, which helps writing the calculation scheme in FORTRAN.

The application of the balance of the boundary conditions is similar, and all are covered in detail in Preissner (2002). In summary, it is seen that boundary conditions #1–#3 and #20–#25 (those at $s=0$ and $x=0$, respectively) could be applied so that they "zero out" certain terms of the power series. However, to keep the forms of all the power series consistent, these boundary conditions are applied as constraints to the potential energy expression. Therefore, the "matching" boundary conditions #1–#19 on "s" each generate $(N+1)$ constraints, while the boundary conditions #20–#35 on "x" each generate $(M+1)$ constraints. The total number of unknown trial function coefficients is therefore $10(M+1)(N+1)$, while the total number of constraint equations on the potential energy expression is $[19(N+1)+16(M+1)]$. If a fifth-order polynomial were taken in each direction, this would result in a system of 360 equations in 360 unknowns that includes 210 constraints.

6. Development of the potential energy expression

The expression for the total potential energy is now needed. Two expressions, one each for the flat and curved parts, are combined and integrated with respect to s and x over their respective bounds. Neglecting any B_{ij}, $(\ )_{16}$, $(\ )_{26}$, or $(\ )_{45}$ coupling in the structure, the expression for the potential energy of the flat plate portion is taken from Eq. (5.70) in Vinson (1999), while the expression for the circular shell corner is taken from Eq. (4.20) in Preissner (2002). Using the strain–displacement relations of Eqs. **?**(4) and (5), the total expression is therefore:

$$
\begin{aligned}
V = \int_0^L \int_0^{S_1} \Bigg\{ & \frac{A_{11}}{2}\left(\frac{\partial u_1}{\partial x}\right)^2 + \frac{D_{11}}{2}\left(\frac{\partial \bar{\beta}_{x_1}}{\partial x}\right)^2 + A_{12}\frac{\partial u_1}{\partial x}\frac{\partial v_1}{\partial s} + D_{12}\frac{\partial \bar{\beta}_{x1}}{\partial x}\frac{\partial \bar{\beta}_{s_1}}{\partial s} + \frac{A_{22}}{2}\left(\frac{\partial v_1}{\partial s}\right)^2 \\
& + \frac{D_{22}}{2}\left(\frac{\partial \bar{\beta}_{s_1}}{\partial s}\right)^2 + A_{55}\left[\frac{1}{2}\left(\bar{\beta}_{x1}\right)^2 + \bar{\beta}_{x_1}\frac{\partial w_1}{\partial x} + \frac{1}{2}\left(\frac{\partial w_1}{\partial x}\right)^2\right] \\
& + A_{44}\left[\frac{1}{2}\left(\bar{\beta}_{s_1}\right)^2 + \bar{\beta}_{s_1}\frac{\partial w_1}{\partial s} + \frac{1}{2}\left(\frac{\partial w_1}{\partial s}\right)^2\right] + A_{66}\left[\frac{1}{2}\left(\frac{\partial u_1}{\partial s}\right)^2 + \frac{\partial u_1}{\partial s}\frac{\partial v_1}{\partial x} + \frac{1}{2}\left(\frac{\partial v_1}{\partial x}\right)^2\right] \\
& + D_{66}\left[\frac{1}{2}\left(\frac{\partial \bar{\beta}_{x_1}}{\partial s}\right)^2 + \frac{\partial \bar{\beta}_{x_1}}{\partial s}\frac{\partial \bar{\beta}_{s_1}}{\partial x} + \frac{1}{2}\left(\frac{\partial \bar{\beta}_{s_1}}{\partial x}\right)^2\right]\Bigg\} \mathrm{d}s\,\mathrm{d}x + \int_{S_1}^{S_2}\int_0^L \Bigg\{ \frac{A_{11}}{2}\left(\frac{\partial u_2}{\partial x}\right)^2 + \frac{D_{11}}{2}\left(\frac{\partial \bar{\beta}_{x_2}}{\partial x}\right)^2 \\
& + A_{12}\left[\left(\frac{\partial u_2}{\partial x}\right)\left(\frac{\partial v_2}{\partial s}\right) + \left(\frac{\partial u_2}{\partial x}\right)\left(\frac{w_2}{R}\right)\right] + D_{12}\left(\frac{\partial \bar{\beta}_{x_2}}{\partial x}\right)\left(\frac{\partial \bar{\beta}_{s_2}}{\partial s}\right) \\
& + \frac{A_{22}}{2}\left[\left(\frac{\partial v_2}{\partial s}\right)^2 + 2\left(\frac{\partial v_2}{\partial s}\right)\left(\frac{w_2}{R}\right) + \left(\frac{w_2}{R}\right)^2\right] + \frac{D_{22}}{2}\left(\frac{\partial \bar{\beta}_{s_2}}{\partial s}\right)^2 \\
& + \frac{A_{66}}{2}\left[\left(\frac{\partial v_2}{\partial x}\right)^2 + 2\left(\frac{\partial v_2}{\partial x}\right)\left(\frac{\partial u_2}{\partial s}\right) + \left(\frac{\partial u_2}{\partial s}\right)^2\right] + \frac{D_{66}}{2}\left[\left(\frac{\partial \bar{\beta}_{s_2}}{\partial x}\right)^2 + 2\left(\frac{\partial \bar{\beta}_{s_2}}{\partial x}\right)\left(\frac{\partial \bar{\beta}_{x_2}}{\partial s}\right) + \left(\frac{\partial \bar{\beta}_{x_2}}{\partial s}\right)^2\right] \\
& + \frac{A_{44}}{2}\left[(\bar{\beta}_{s_2})^2 + 2(\bar{\beta}_{s_2})\left(\frac{\partial w_2}{\partial s}\right) - 2\left(\bar{\beta}_{s_2}\right)\left(\frac{v_2}{R}\right) + \left(\frac{\partial w_2}{\partial s}\right)^2 - 2\left(\frac{\partial w_2}{\partial s}\right)\left(\frac{v_2}{R}\right) + \left(\frac{v_2}{R}\right)^2\right] \\
& + \frac{A_{55}}{2}\left[\left(\bar{\beta}_{x_2}\right)^2 + 2\left(\bar{\beta}_{x_2}\right)\left(\frac{\partial w_2}{\partial x}\right) + \left(\frac{\partial w_2}{\partial x}\right)^2\right]\Bigg\} \mathrm{d}x\,\mathrm{d}s - \int_0^L \int_0^{S_1} p_i w_1\,\mathrm{d}s\,\mathrm{d}x - \int_0^L \int_{S_1}^{S_2} p_i w_2\,\mathrm{d}s\,\mathrm{d}x
\end{aligned}
\tag{21}
$$

Using Eq. (6), Eq. (21) is subsequently expressed in terms of the power series assumed for the displacements. Once all terms have been expressed as power series and integrated, they are substituted back into the potential energy expression. An overview of the substitution and integration process, and the resulting potential energy expression is shown in Appendix A; full details are given in Preissner (2002).

7. Application of the quadratic programming method for solution

Looking at the overall problem with a broad focus shows that this effort falls under the larger category of optimization. Specifically, with an objective function (V) that is quadratic, and with constraints that are

only linear, this specific problem is one of quadratic programming. (see e.g., Chapter 10 of Fletcher (1981), or Gill and Murray (1974).)

In the two-dimensional analysis, the authors had used the IMSL Math Library (double precision) routine DLSLSF to solve the real, linear, and symmetric system of $\mathbf{Ax} = \mathbf{b}$ (Anonymous, 1994) that resulted after setting $\delta(V) = 0$. Now we turn to the IMSL (double precision) routine DQPROG. The IMSL documentation regarding this routine is a bit sparse, but fortunately, Chapter 10 of Fletcher (1981) describes the exact problem DQPROG solves, and even gives an example on pg. 81. Formally, this is an optimization problem in which the objective function $f(\mathbf{x})$ is quadratic (i.e., V) and the constraint functions $c_i(\mathbf{x})$ are linear. Quadratic programming differs from linear programming in that it is possible to have meaningful problems in which there are no inequality constraints. Thus, the problem is to find a solution $\mathbf{x}^*$ to the equality constraint problem:

$$\min_{\mathbf{x}} q(\mathbf{x}) \equiv \frac{1}{2}\mathbf{x}^{\mathrm{T}}\mathbf{H}\mathbf{x} + \mathbf{g}^{\mathrm{T}}\mathbf{x} \tag{22}$$

subject to the constraints:

$$\mathbf{A}^{\mathrm{T}}\mathbf{x} = \mathbf{b} \tag{23}$$

The matrix $\mathbf{H}$ is defined as the Hessian (the matrix of second partial derivatives) of the objective function.

To complete the problem, a FORTRAN program is written to calculate and fill in the coefficients of the $\mathbf{H}$ and $\mathbf{A}$ matrices and the $\mathbf{g}$ and $\mathbf{b}$ vectors. This information is then passed to the particular IMSL routine, DQPROG, which solves the system. Details of the specific implementation of this routine can be found in the IMSL documentation (Anonymous, 1994).

To ensure that the input and output of the FORTRAN program is ordered and consistent, a numbering scheme for the coefficients (variables) and constraints was developed. There are ten different sets of variables (one set for each power series expansion), and the number of variables in each set and the number of constraints both vary with the powers of the series in each direction. Because of this, the numbering scheme is somewhat complicated. The full details of this scheme are not included here, but can be found in Preissner (2002). Such detailed organization is required so that proper deflections, strains, and stresses are calculated with the solution.

Because the calculations of the coefficients of the Hessian matrix $\mathbf{H}$ are rather involved, there is a separate subroutine for each power series. The row and column number of any one component of $\mathbf{H}$ is determined by the two variables in the second partial derivative. For example, in the $k_{i,j}$ section, there will be the term $\partial^2 V/\partial k_{i,j}\partial p_{k,l}$. In any particular analysis, there will be definite values for the powers of the expansions (M, N) and the dummy indices (i, j, k, l). The numbering scheme uses these values to determine a unique number for each variable, i.e., for each combination of power series (a, b, c, etc.) and M, N, i, j, k, and l. Therefore, the row and column of any particular term is determined by the two unique identifying numbers of the variables in the denominator. These are continuous functions so that by symmetry, the coefficient in the location corresponding to $\partial^2 V/\partial p_{k,l}\partial k_{i,j}$ would be the same.

In the quadratic programming method of solution, the constraint equations are not explicitly included in the potential energy expression. They are accounted for in the optimization process by their inclusion in the $\mathbf{A}$ constraint matrix. Thus each constraint must also have a unique number, as this becomes the row number of the constraint within the $\mathbf{A}$ matrix. As seen previously, the number of constraints also varies with the powers of the series expansions, similar to the variable numbers. The constraint numbering scheme is detailed in Preissner (2002) as well. Each constraint contains various unknown expansion coefficients. The unique identifying number of the particular unknown(s) appearing in the constraint gives the column in $\mathbf{A}$ for entering their respective coefficients. The constraint matrix $\mathbf{A}$ will not be symmetric. As all of the constraints are equal to zero, the $\mathbf{b}$ vector is easily filled and becomes the null vector, $\mathbf{0}$.

The **g** vector will be filled with the coefficients of the linear terms of the potential energy expression. This will be the pressure loading terms in this case, and will only apply to the $a_{i,j}$ and $b_{i,j}$ variables (all others positions will be equal to zero). The index of the coefficient within **g** (i.e., its row number) will be determined as above.

As an example of generating the components of **H**, find $\partial V/\partial a_{i,j}$ (Note: in the following, the summation signs are retained to indicate the range of the index variables. For each partial derivative term, only one combination of the indices i, j, k, and l is appropriate, not the entire summation.):

$$\begin{aligned}\frac{\partial V}{\partial a_{i,j}} &= 2\left[\frac{A_{44}}{2}\sum_{i=1}^{M}\sum_{j=0}^{N}\frac{(i^2)S_1^{2i-1}L^{2j+1}}{(2i-1)(2j+1)}+\frac{A_{55}}{2}\sum_{i=0}^{M}\sum_{j=1}^{N}\frac{(j^2)S_1^{2i+1}L^{2j-1}}{(2i+1)(2j-1)}\right]a_{i,j}\\ &+\left[A_{44}\sum_{i=1}^{M}\sum_{j=0}^{N}\sum_{\substack{k=i\\k>i}}^{M}\sum_{\substack{l>j\\l=0}}^{N}\frac{(ik)S_1^{i+k-1}L^{j+l+1}}{(i+k-1)(j+l+1)}+A_{55}\sum_{i=0}^{M}\sum_{j=1}^{N}\sum_{\substack{k=i\\k>i}}^{M}\sum_{\substack{l>j\\l=1}}^{N}\frac{(jl)S_1^{i+k+1}L^{j+l-1}}{(i+k+1)(j+l-1)}\right]a_{k,l}\\ &+\left[A_{44}\sum_{i=1}^{M}\sum_{j=0}^{N}\sum_{k=0}^{M}\sum_{l=0}^{N}\frac{(i)S_1^{i+k}L^{j+l+1}}{(i+k)(j+l+1)}\right]k_{k,l}+\left[A_{55}\sum_{i=0}^{M}\sum_{j=1}^{N}\sum_{k=0}^{M}\sum_{l=0}^{N}\frac{(j)S_1^{i+k+1}L^{j+l}}{(i+k+1)(j+l)}\right]p_{k,l}\\ &-p_i\sum_{i=0}^{M}\sum_{j=0}^{N}\frac{S_1^{i+1}L^{j+1}}{(i+1)(j+1)}\end{aligned} \tag{24}$$

Next, find the second derivatives (recalling that, because they are continuous, the order of differentiation does not matter, i.e., $\partial^2 V/\partial p_i\,\partial p_j = \partial^2 V/\partial p_j\,\partial p_i$):

$$\frac{\partial^2 V}{\partial a_{i,j}^2} = 2\left[\frac{A_{44}}{2}\sum_{i=1}^{M}\sum_{j=0}^{N}\frac{(i^2)S_1^{2i-1}L^{2j+1}}{(2i-1)(2j+1)}+\frac{A_{55}}{2}\sum_{i=0}^{M}\sum_{j=1}^{N}\frac{(j^2)S_1^{2i+1}L^{2j-1}}{(2i+1)(2j-1)}\right] \tag{25}$$

$$\frac{\partial^2 V}{\partial a_{i,j}\,\partial a_{k,l}} = \left[A_{44}\sum_{i=1}^{M}\sum_{j=0}^{N}\sum_{\substack{k=i\\k>i}}^{M}\sum_{\substack{l>j\\l=0}}^{N}\frac{(ik)S_1^{i+k-1}L^{j+l+1}}{(i+k-1)(j+l+1)}+A_{55}\sum_{i=0}^{M}\sum_{j=1}^{N}\sum_{\substack{k=i\\k>i}}^{M}\sum_{\substack{l>j\\l=1}}^{N}\frac{(jl)S_1^{i+k+1}L^{j+l-1}}{(i+k+1)(j+l-1)}\right] \tag{26}$$

$$\frac{\partial^2 V}{\partial a_{i,j}\,\partial k_{k,l}} = \left[A_{44}\sum_{i=1}^{M}\sum_{j=0}^{N}\sum_{k=0}^{M}\sum_{l=0}^{N}\frac{(i)S_1^{i+k}L^{j+l+1}}{(i+k)(j+l+1)}\right] \tag{27}$$

$$\frac{\partial^2 V}{\partial a_{i,j}\,\partial p_{k,l}} = \left[A_{55}\sum_{i=0}^{M}\sum_{j=1}^{N}\sum_{k=0}^{M}\sum_{l=0}^{N}\frac{(j)S_1^{i+k+1}L^{j+l}}{(i+k+1)(j+l)}\right] \tag{28}$$

All other components in the $a_{i,j}$ row/column will be zero. Note that if $M = N = 2$, then there will be nine $a_{i,j}$ coefficients: $a_{0,0}$, $a_{0,1}$, $a_{0,2}$, $a_{1,0}$, $a_{1,1}$, $a_{1,2}$, $a_{2,0}$, $a_{2,1}$, and $a_{2,2}$. For each of these nine coefficients, there would

be multiple versions of Eqs. (25)–(28). This process is performed similarly for the other unknown coefficients.

A FORTRAN program, approximately 2700 lines long, was written to implement this method and calculate the solution. The program consists of a main routine and 14 subroutines. The main routine controls the flow of the program and input and output. Input to the program is by a separate ASCII input file using namelist variables, and controls most aspects of the calculation. Output is to a formatted ASCII file.

After a solution is generated, information regarding the solution is output. This includes the values of the unknowns, the number of active constraints (i.e., constraints that actually "constrained" the solution), the corresponding constraint numbers for the active constraints, and the values of the Lagrange multipliers for the active constraints. A separate subroutine is then called which uses the generated solution to calculate the values of the constraints as they are mathematically described. These calculations confirm whether the constraints were met as intended, and the routine outputs the exact values of the constraints (as calculated with solution coefficients) to the file.

The final step in the program is to use the coefficients found above to calculate and output the deflections, rotations, and stresses. Loops in the main program set the (s,x) location and then call a subroutine to calculate and output the relevant quantities at that spatial location. The values of the deflections, etc. are not stored in matrices, but rather are calculated on the spot and output immediately. Two loops are used, one to calculate quantities at constant "s" locations, the other to calculate quantities at constant "x" locations. Quantities are calculated at three constant s-locations; at or near $s = 0$, at or near $s = S_1$, and at or near $s = S_2$. For each constant s-location, the quantities are calculated at 101 x-locations. Quantities are subsequently also calculated at or near nine constant x-locations, evenly distributed along the length of the shell (including the very ends). For each constant x-location, the quantities are calculated at 51 points for $0 \leqslant s \leqslant S_1$ and at 50 points for $S_1 < s \leqslant S_2$.

For each loop that determines a specific (s,x) location, each power series and its derivatives must be summed for all powers of s and x, i.e., from $0 \rightarrow M$ for s and $0 \rightarrow N$ for x. These summation loops take place in the subroutine that calculates the deflections and stresses. These summations are somewhat tricky, as all power series coefficients are numbered consecutively in the output solution matrix, yet they must also increment from the beginning of any one power series to obtain the correct summation. Once the deflections and their derivatives are calculated, the strains in the structure are calculated, and subsequently the stresses are found through matrix multiplication of the strain matrix and the $\overline{\mathbf{Q}}$ stiffness matrix.

Note also that to match ABAQUS (or other finite element) stress results, stresses must be calculated at the same (s,x) location as the integration point for the finite element. This means that stresses can not be compared exactly at $s = 0$, S_1, and S_2 if the finite element grid is symmetric every 45°. For example, if $S_1 = 2.0$ and $R = 1.5$, then $S_2 = S_1 + (2\pi R/8) \cong 3.1781$. If there are eight elements from S_1 to S_2, and the integration point is in the middle of the element, then stresses should be calculated at $s = S_2 - [(S_2 - S_1)/16] = 3.1045$. Of course, if the integration point is at a different location, this calculation would need to be adjusted. Thus, all of the derivatives are calculated at the stress point, along with the quantities w_2, v_2, $\bar{\beta}_{x_1}$, $\bar{\beta}_{s_1}$, $\bar{\beta}_{x_2}$, $\bar{\beta}_{s_2}$, which are calculated at both points.

8. Finite element analysis

The MPE analysis was compared to ABAQUS finite element analyses using both shell and continuum or "brick" elements. Due to the lack of external experimental data, the continuum finite element analysis is taken to be the "truth" for this study, as the formulation of such continuum elements is based on full three-dimensional elasticity, without assumptions or neglect of phenomena.

As with shell elements, ABAQUS has numerous types of continuum elements available. Selection criteria for continuum elements are covered in detail in Section 14.1.1 of the ABAQUS User's Manual (Anonymous, 1997). Based on these choices, the C3D20R element was used. This is a second-order, reduced integration brick element with 20 nodes. Each node has three displacement degrees of freedom. The shell element was the S4R four-node, doubly curved element used in Part I. Each node has three displacement and three rotation degrees of freedom. It is noted that continuum elements are not inherently more accurate for composite structures than shell elements. However, continuum elements are preferred when transverse shear effects are significant, when normal stress can not be neglected, or when accurate interlaminar stresses are required.

During the finite element analyses, grid refinement studies were performed to ensure a converged solution. Depending on the length of the shell, final model sizes ranged between ~250,000 and 1.1 million degrees of freedom. As a check case, a true circular cylinder was modeled with both ABAQUS and the MPE method. The results showed good agreement between the two methods, as well as with the classic Timoshenko solution (Timoshenko and Woinowsky-Krieger, 1959).

9. Results and discussion

The specific physical problem examined is the same as that used in Part I (Preissner and Vinson, 2002a), with the addition of the length dimension. A short shell of 5.0 m and a long shell of 50.0 m in length were analyzed. The cross-section had 4.0 m flat sides connected with circular arc corners of 2.0 m radius. The material was a graphite/foam core sandwich of T300/5208 carbon/epoxy and Klegecell foam. The skin thickness was 5.0 mm and the core thickness was 20 cm. A constant internal pressure of 0.1 MPa was applied. Specific material properties can be found in the results and discussion section of Part I.

The presented results are the best that were obtainable with the current MPE formulation and solution methodology. This "best" is as compared to the finite element results; that is, the best MPE results are those that matched the finite element results the closest. To do this, a range of power series orders was examined, from $M = N = 3$ to $M = N = 10$. Studies were also performed where $M \neq N$, but the best results were when $M = N$. It was found that at first the results converged with increasing series order, but that above a certain order they diverged or tended to zero. For the short shells, this occurred after the MPE results had matched the finite element results. For the long shells, this was not the case, and even the best results are a poor

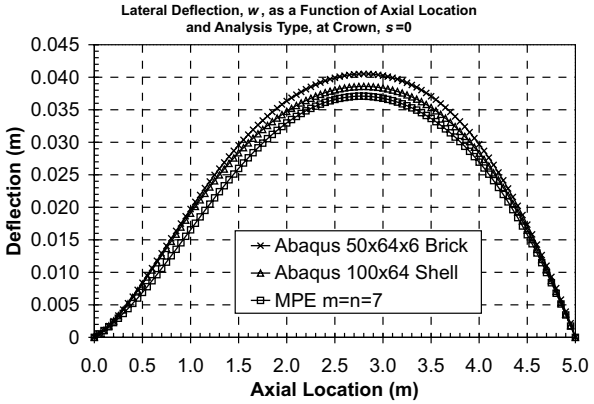

Fig. 3. Comparison of lateral deflection, w, all methods, $L = 5$ m, $s = 0.0$.

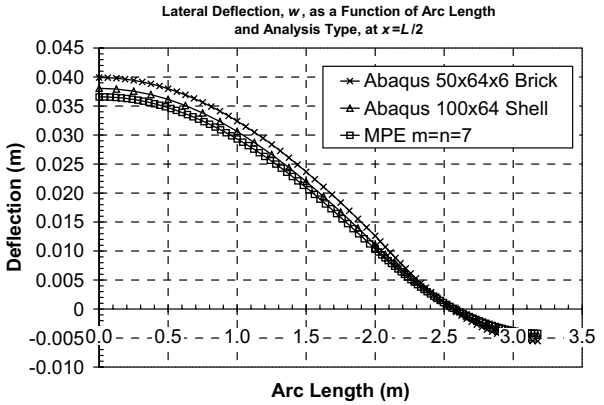

Fig. 4. Comparison of lateral deflection, w, all methods, $L = 5$ m, $x = L/2$.

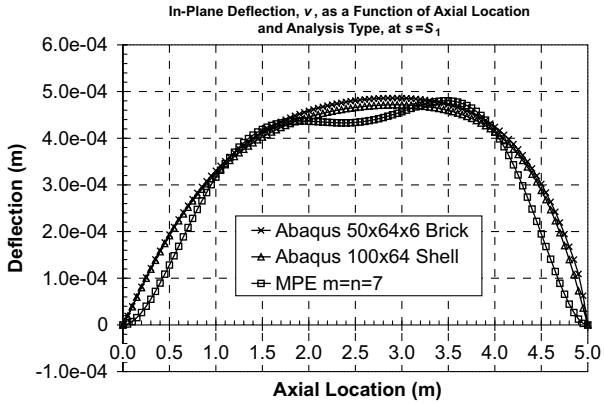

Fig. 5. Comparison of in-plane deflection, v, all methods, $L = 5$ m, $s = S_1$.

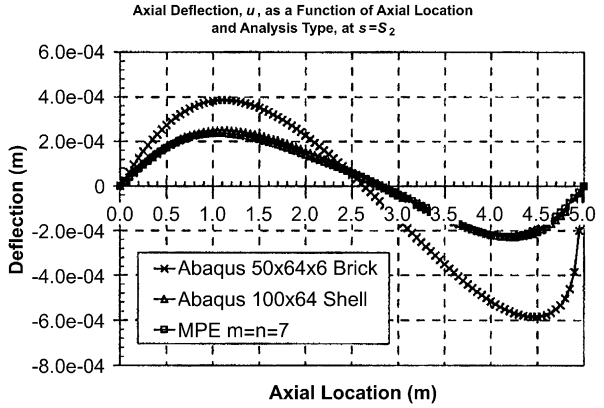

Fig. 6. Comparison of axial deflection, u, all methods, $L = 5$ m, $s = S_2$.

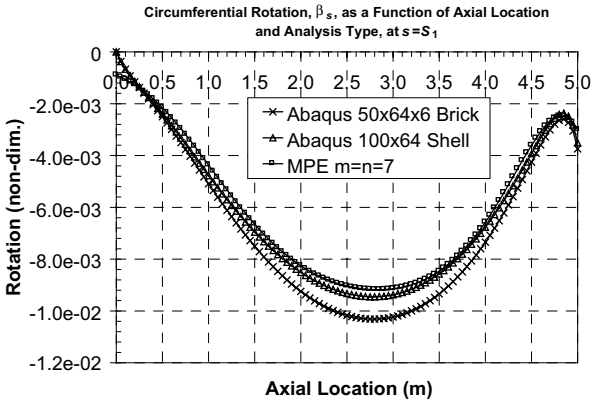

Fig. 7. Comparison of circumferential rotation, β_s, all methods, $L = 5$ m, $s = S_1$.

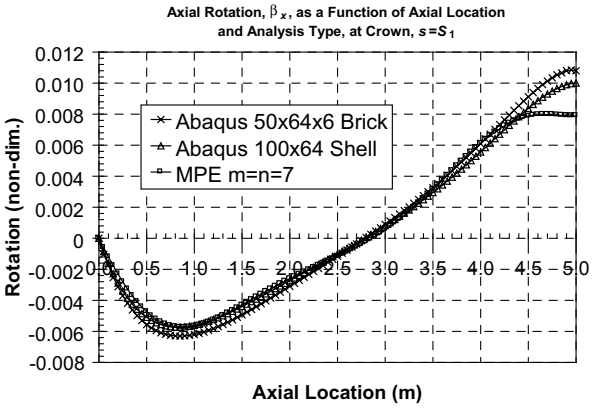

Fig. 8. Comparison of axial rotation, β_x, all methods, $L = 5$ m, $s = S_1$.

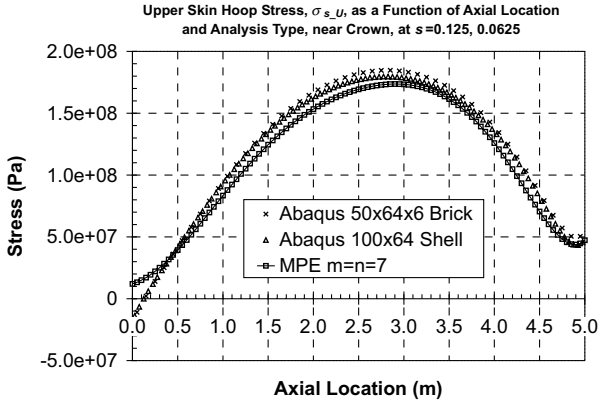

Fig. 9. Comparison of upper skin hoop stress, σ_s, all methods, $L = 5$ m, $s \cong 0.0$.

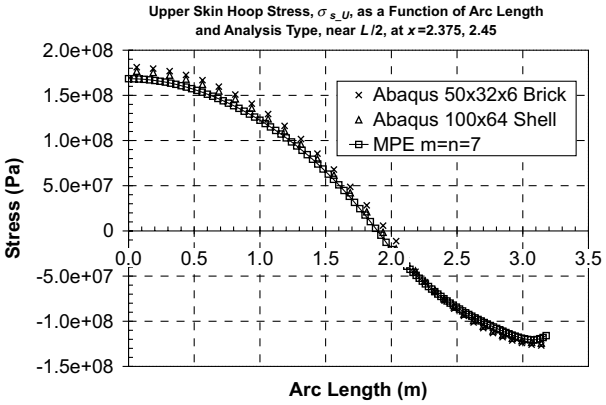

Fig. 10. Comparison of upper skin hoop stress, σ_s, all methods, $L = 5$ m, $x \cong L/2$.

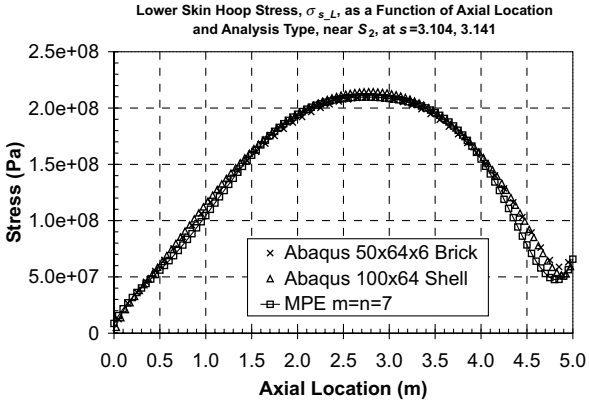

Fig. 11. Comparison of lower skin hoop stress, σ_s, all methods, $L = 5$ m, $s \cong S_2$.

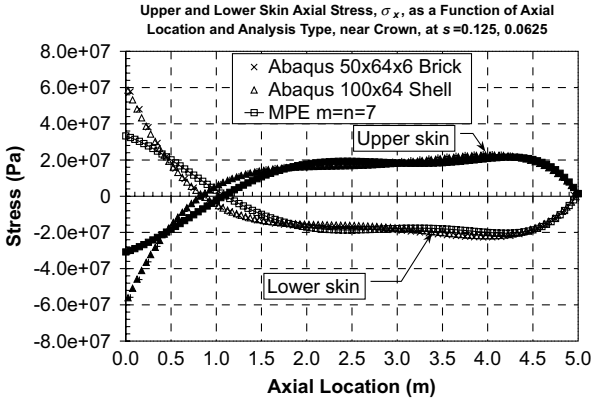

Fig. 12. Comparison of skin axial stress, σ_x, all methods, $L = 5$ m, $s \cong 0.0$.

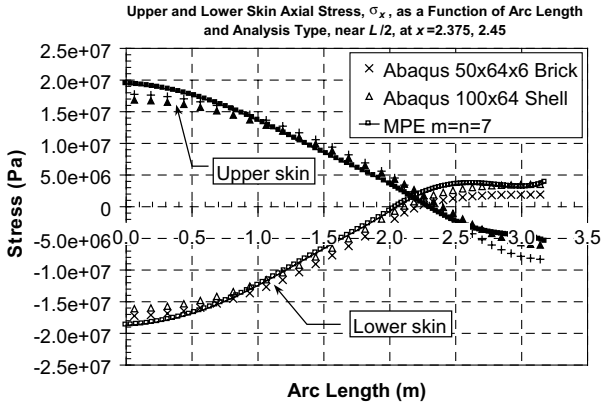

Fig. 13. Comparison of skin axial stress, σ_x, all methods, $L = 5$ m, $x \cong L/2$.

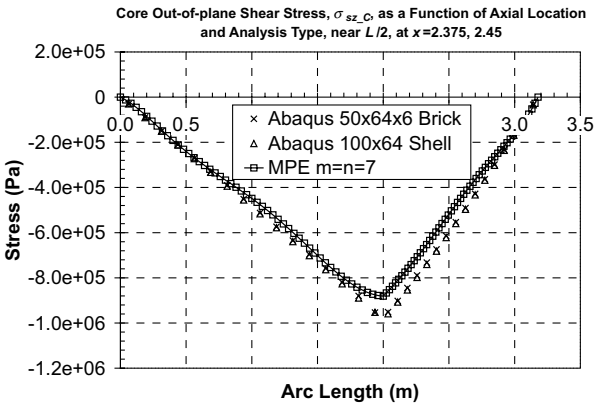

Fig. 14. Comparison of core shear stress, σ_{sz}, all methods, $L = 5$ m, $x \cong L/2$.

match to the finite elements. Based on their similar variational formulations, better correlation was expected. More investigation is needed to determine exactly why the MPE method broke down for long shells.

9.1. "Short" shell, L = 5 m

Comparisons of selected deflections are given in Figs. 3–8, and comparisons of selected stresses are provided in Figs. 9–14. It is seen from these figures that the finite element analyses and the MPE method do indeed give very similar answers. However, the MPE results results are closer to the "shell" analysis than to the brick analysis (except near clamped end). This is because the MPE and shell analyses are closer in formulation, due to their neglect of σ_z and inclusion of the rotations, than are the shell and brick formulations. The brick formulation predicts the largest deflections and consequently the largest stresses, but the difference in stresses is not as large as the difference in deflections might lead one to think. This result is in line with the fact that the brick formulation is more complex with more degrees of freedom.

The largest difference between the MPE and FEM results are at the ends. This disparity is due to the difference in the implementation of the boundary conditions in the methods. The MPE method used theoretical boundary conditions that included force constraints. The FEM analyses have no force conditions, and use only restrictions on displacements.

Unsurprisingly, the largest deflections occur near half-length; the largest rotations occur near (not at) the ends. The highest stresses are the hoop stresses, but they are not critical as the ultimate tensile and compressive strength in the fiber direction is 1.5 GPa (1.5×10^9 Pa). The upper and lower skin exchange roles; at $s = 0$ the upper skin is in tension, while the lower skin is in compression; at $s = S_2$ the roles are reversed. The hoop stress levels are ~10% of ultimate strength, but due to the compressive loading, the buckling of the inner face in the corner should be examined. It turns out that the skin axial stress is critical for this structure, as it is (an unrealistic) 100% hoop wrap (see Fig. 12). The ultimate strength of the carbon/epoxy is only 4×10^7 Pa in tension transverse to the fibers, and this is exceeded at the clamped end in the

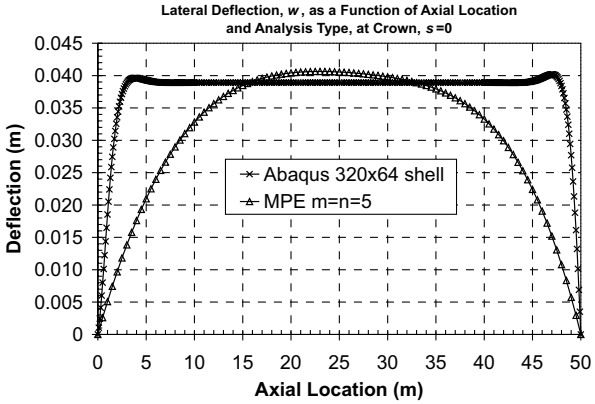

Fig. 15. Comparison of lateral deflection, w, all methods, $L = 50$ m, $s = 0.0$.

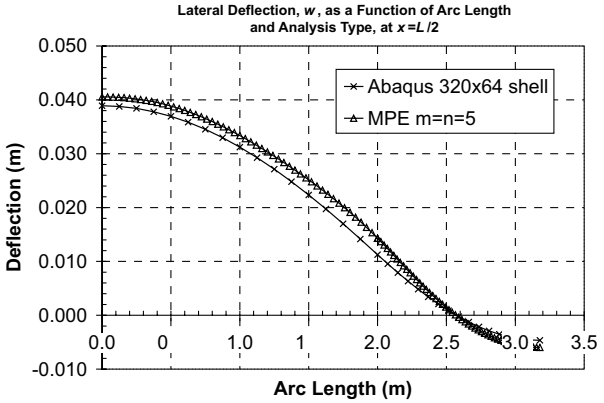

Fig. 16. Comparison of lateral deflection, w, all methods, $L = 50$ m, $x = L/2$.

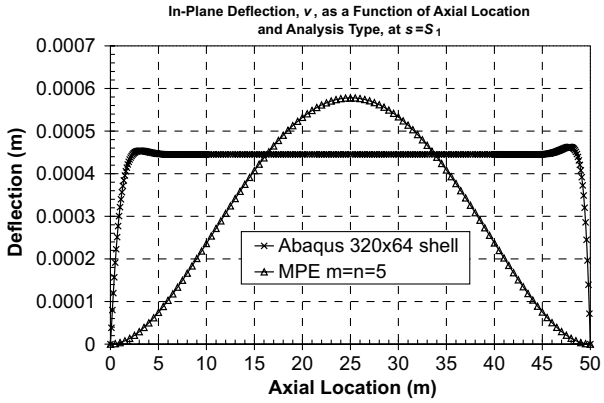

Fig. 17. Comparison of in-plane deflection, v, all methods, $L = 50$ m, $s = S_1$.

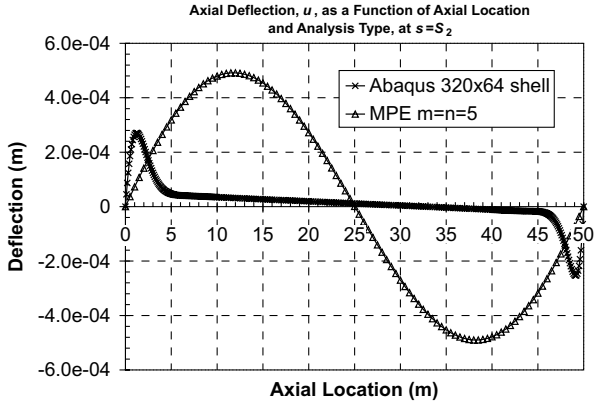

Fig. 18. Comparison of axial deflection, u, all methods, $L = 50$ m, $s = S_2$.

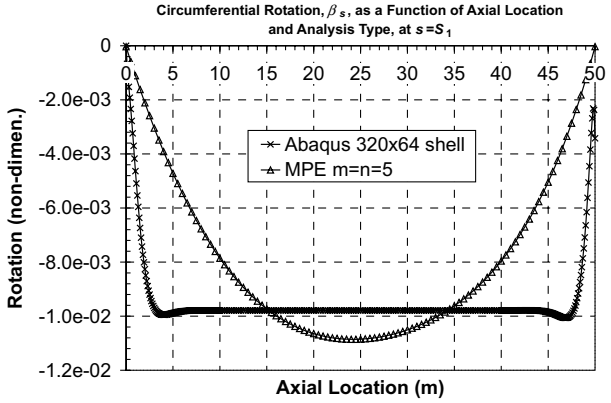

Fig. 19. Comparison of circumferential rotation, β_s, all methods, $L = 50$ m, $s = S_1$.

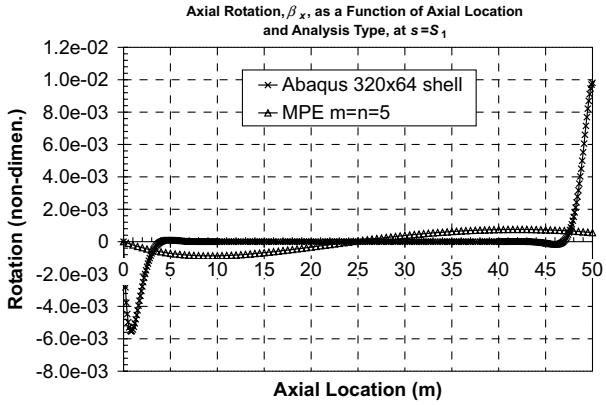

Fig. 20. Comparison of axial rotation, β_x, all methods, $L = 50$ m, $s = S_1$.

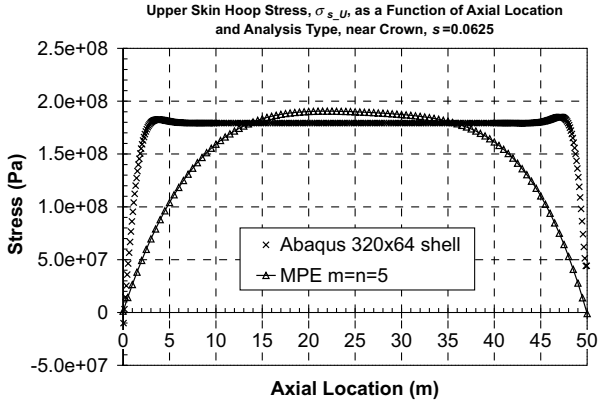

Fig. 21. Comparison of upper skin hoop stress, σ_s, all methods, $L = 50$ m, $s \cong 0.0$.

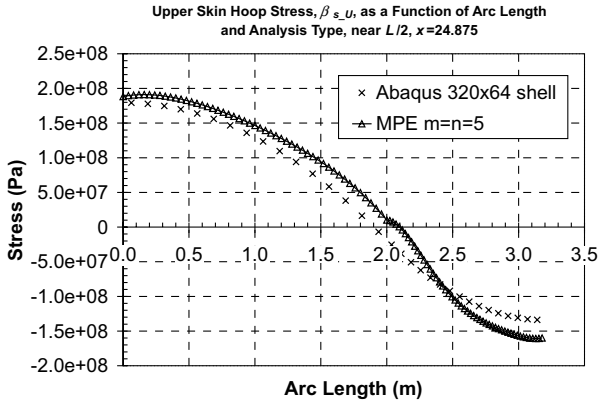

Fig. 22. Comparison of upper skin hoop stress, σ_s, all methods, $L = 50$ m, $x \cong L/2$.

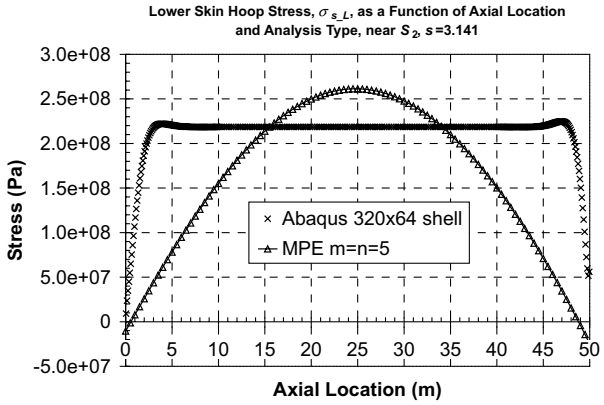

Fig. 23. Comparison of lower skin hoop stress, σ_s, all methods, $L = 50$ m, $s \cong S_2$.

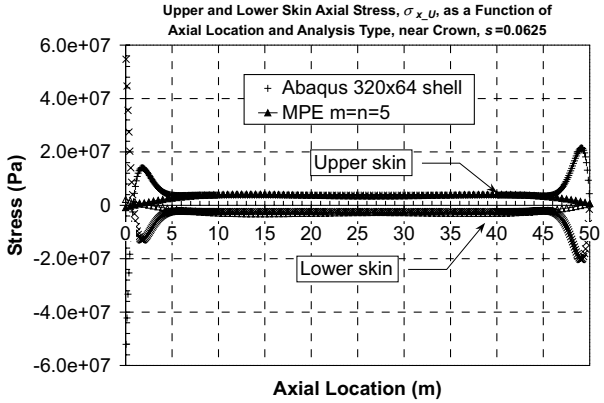

Fig. 24. Comparison of skin axial stress, σ_x, all methods, $L = 50$ m, $s \cong 0.0$.

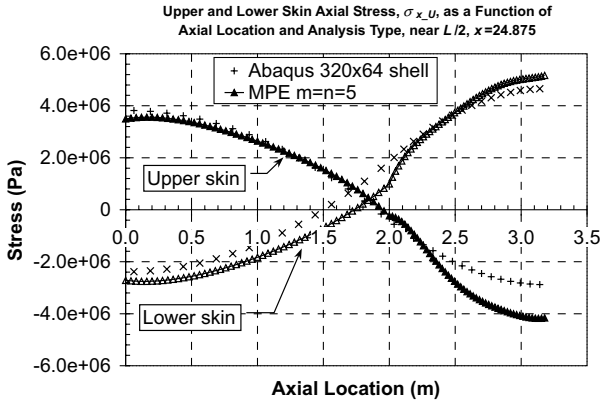

Fig. 25. Comparison of skin axial stress, σ_x, all methods, $L = 50$ m, $x \cong L/2$.

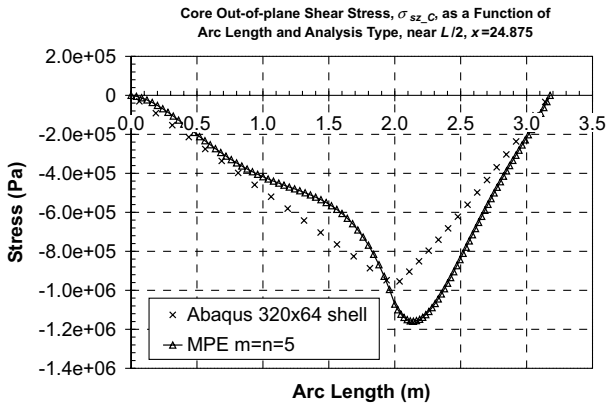

Fig. 26. Comparison of core shear stress, σ_{sz}, all methods, $L = 50$ m, $x \cong L/2$.

FEM analyses. This figure also points up the significant influence of the boundary conditions, where the MPE boundary conditions are such that the skin stays below its ultimate strength. Stresses at the clamped end are seen to be much greater than at simply supported end, due to the greater restriction. Hoop stresses are not as affected by the differing boundary conditions.

9.2. "Long" shell, L = 50 m

For this case, deflection results are shown in Figs. 15–20, and stress results are shown in Figs. 21–26. These figures are directly comparable to those in Figs. 3–8 and 9–14, in both parameter and location examined. However, only shell analysis results are used for comparison in this instance, as these results adequately reflect the differences between the MPE and FEM methods.

Even a cursory examination of the plots shows that the agreement between the MPE and FEM results is not satisfactory. In particular, the MPE results do a very poor job of capturing the behavior of the shell near the ends. For many parameters, the MPE results come closest to the FEM values only in a short axial extent near the middle of the overall length (i.e., in the "membrane" response section of the shell). In that area, the MPE results capture the general circumferential variation of parameters; a constant axial slice at $x = L/2$ such as in Fig. 16 shows reasonable agreement. However, variations along the length (e.g., Figs. 17, 19, 20 or 23) or other variations in circumference (e.g., Fig. 25) show poor overall correlation.

As with the deflections, the MPE results do a poor job of capturing the axial variation of the stresses near the ends of the shell. However, in the (membrane) region 15 m $< x <$ 35 m, the MPE results are reasonably (but not satisfactorily) close to the FEM results. Figs. 24 and 21 show moderate axial agreement in the central section, while Figs. 22 and 26 show reasonable agreement in the circumferential direction at $x = L/2$.

10. Conclusions

As developed for this research, the method provided good accuracy in two dimensions and for short three-dimensional shells. However, for longer shells, the MPE method could not capture the essential bending boundary layer behavior of such structures. It is felt that this is not an inherent limitation in the

MPE method, but is perhaps a combination of non-optimal choice of displacement functions and/or a solver that was overwhelmed by the number of variables.

It seems higher order power series are needed to properly capture the strong variations of parameters within the bending boundary layer. The number of unknown variables increases as the square of the power series order. For the long shells and higher order series, the DQPROG function failed to reach a solution. This points out the difficulties in using a pre-written solution routine: the source code was unavailable, and the documentation and diagnostic outputs were inadequate to identify the problem(s). More robust solvers can be examined in future efforts.

In addition, while the current solution method allows the use of functions that do not a priori meet the boundary conditions, such a choice was seen to make the problem more complex. Soldatos and Messina (1998) point out that the basis functions used to represent the displacements should be a complete and orthonormal set, for best numerical performance. This will be explored in future research.

As formulated, the MPE method is a reasonably useful tool for rapidly screening ideas and concepts for different cross-sectional shapes (in two dimensions). To the authors' knowledge, this is a unique application of the MPE method, and it met most goals set out at the beginning of the research.

Despite the unsatisfactory performance on the longer shells, some positive conclusions can be made about the MPE method: (1) as it uses continuous functions, it allows for the determination of displacements and stresses at any location in the body; (2) the development of such an analytical method can give one a greater physical insight into the problem that "canned" analysis tools can not; and (3) once developed, it was easier and faster to change parameters (within the range of the formulation) than with finite elements. The flexibility of the FORTRAN program and the use of continuous functions allowed for a tailorable level of data output.

In addition to the difficulties with the long shells, the MPE method had the following weaknesses: (1) as currently implemented, it lacks the flexibility to go beyond the limited range of geometric parameters that it was developed for; (2) it does not include the important effects of transverse normal stress and structural coupling (i.e., B_{ij}, etc.), (3) a better method for determining convergence and/or error analysis is needed, and (4) initial development of the method was labor intensive. However, with the foundation of the research that has already been completed, these issues could be addressed in an effective fashion.

As a final note, this research was also a unique analysis of an unconventional structural shape. The analysis uncovered interesting bending boundary layer behavior that is not explained by classical bending boundary layer ideas. This boundary layer behavior is more fully explored in a separate paper that deals with a trade study on the fundamental geometric parameters of the shell (Preissner and Vinson, 2002b).

Acknowledgements

This work was supported by the United States Navy Office of Naval Research, contracts #30-12420-037-62112 and #N00014-97-1-0638.

Appendix A

Eq. (21) must be expressed in terms of the power series assumed for the displacements. As an example, the first term is worked out:

$$\left(\frac{\mathrm{d}u_1}{\mathrm{d}x}\right)^2 = \left(\sum_{i=0}^{M}\sum_{j=1}^{N} j f_{i,j} s^i x^{j-1}\right)^2 \tag{A.1}$$

The product of two, two-variable power series can be given by:

$$f(s,x)\cdot g(s,x)=\left(\sum_{i=0}^{M}\sum_{j=0}^{N}a_{i,j}s^{i}x^{j}\right)\left(\sum_{k=0}^{M}\sum_{l=0}^{N}b_{k,l}s^{k}x^{l}\right)=\sum_{i=0}^{M}\sum_{j=0}^{N}\sum_{k=0}^{M}\sum_{l=0}^{N}a_{i,j}b_{k,l}s^{i+k}x^{j+l} \tag{A.2}$$

If this is a "squared" product, then this can be simplified:

$$\begin{aligned}[f(s,x)]^{2}=f(s,x)\cdot f(s,x)&=\left(\sum_{i=0}^{M}\sum_{j=0}^{N}a_{i,j}s^{i}x^{j}\right)\left(\sum_{k=0}^{M}\sum_{l=0}^{N}a_{k,l}s^{k}x^{l}\right)=\sum_{i=0}^{M}\sum_{j=0}^{N}\sum_{k=0}^{M}\sum_{l=0}^{N}a_{i,j}a_{k,l}s^{i+k}x^{j+l}\\&=\sum_{i=0}^{M}\sum_{j=0}^{N}a_{i,j}^{2}s^{2i}x^{2j}+2\sum_{i=0}^{M}\sum_{j=0}^{N}\sum_{\substack{k=i\\ \text{when } k>i}}^{M}\sum_{\substack{l>j\\ \text{then } l=0}}^{N}a_{i,j}a_{k,l}s^{i+k}x^{j+l}\end{aligned} \tag{A.3}$$

Note that the rules for the k and l indices above are: (1) the starting value for the k loop is the value of i for that iteration, and on this starting k loop, the l loop must start out as greater than the value of j, but (2) when k increments to be $>i$, then the l loop must start at whatever value the j loop started at.

Therefore, Eq. (A.1) becomes:

$$\left(\frac{\mathrm{d}u_{1}}{\mathrm{d}x}\right)^{2}=\sum_{i=0}^{M}\sum_{j=1}^{N}j^{2}f_{i,j}^{2}s^{2i}x^{2j-2}+2\sum_{i=0}^{M}\sum_{j=1}^{N}\sum_{\substack{k=i\\ k>i}}^{M}\sum_{\substack{l\geq j\\ l=1}}^{N}jlf_{i,j}f_{k,l}s^{i+k}x^{j+l-2} \tag{A.4}$$

Now, one might as well integrate Eq. (A.4) with respect to x and s:

$$\int_{0}^{L}\int_{0}^{S_{1}}\frac{A_{11}}{2}\left(\frac{\mathrm{d}u_{1}}{\mathrm{d}x}\right)^{2}\mathrm{d}s\,\mathrm{d}x=\frac{A_{11}}{2}\int_{0}^{L}\int_{0}^{S_{1}}\left(\sum_{i=0}^{M}\sum_{j=1}^{N}j^{2}f_{i,j}^{2}s^{2i}x^{2j-2}+2\sum_{i=0}^{M}\sum_{j=1}^{N}\sum_{\substack{k=i\\ k>i}}^{M}\sum_{\substack{l\geq j\\ l=1}}^{N}jlf_{i,j}f_{k,l}s^{i+k}x^{j+l-2}\right)\mathrm{d}s\,\mathrm{d}x$$

The integral thus becomes:

$$\begin{aligned}\int_{0}^{L}\int_{0}^{S_{1}}\frac{A_{11}}{2}\left(\frac{\mathrm{d}u_{1}}{\mathrm{d}x}\right)^{2}\mathrm{d}s\,\mathrm{d}x=\frac{A_{11}}{2}\Bigg(&\sum_{i=0}^{M}\sum_{j=1}^{N}\frac{j^{2}}{(2i+1)(2j-1)}f_{i,j}^{2}S_{1}^{2i+1}L^{2j-1}\\&+2\sum_{i=0}^{M}\sum_{j=1}^{N}\sum_{\substack{k=i\\ k>i}}^{M}\sum_{\substack{l>j\\ l=1}}^{N}\frac{jl}{(i+k+1)(j+l-1)}f_{i,j}f_{k,l}S_{1}^{i+k+1}L^{j+l-1}\Bigg)\end{aligned} \tag{A.5}$$

The subsequent terms in Eq. (21) are handled in a similar fashion. Once all terms have been expressed as power series and integrated, they are substituted back into the potential energy expression. The resulting potential energy expression is shown below. For clarity, dashed lines have been added between major sections; recall also that the comma in the variable subscripts *does not* mean differentiation, but is also used for clarity.

$$V = \left[\frac{A_{44}}{2}\sum_{i=1}^{M}\sum_{j=0}^{N}\frac{(i^2)S_1^{2i-1}L^{2j+1}}{(2i-1)(2j+1)} + \frac{A_{55}}{2}\sum_{i=0}^{M}\sum_{j=1}^{N}\frac{(j^2)S_1^{2i+1}L^{2j-1}}{(2i+1)(2j-1)}\right]a_{i,j}^2$$

$$+ \left[A_{44}\sum_{i=1}^{M}\sum_{j=0}^{N}\sum_{\substack{k=i\\k>i}}^{M}\sum_{\substack{l>j\\l=0}}^{N}\frac{(ik)S_1^{i+k-1}L^{j+l+1}}{(i+k-1)(j+l+1)} + A_{55}\sum_{i=0}^{M}\sum_{j=1}^{N}\sum_{\substack{k=i\\k>i}}^{M}\sum_{\substack{l>j\\l=1}}^{N}\frac{(jl)S_1^{i+k+1}L^{j+l-1}}{(i+k+1)(j+l-1)}\right]a_{i,j}a_{k,l}$$

$$+ \left[A_{44}\sum_{i=1}^{M}\sum_{j=0}^{N}\sum_{k=0}^{M}\sum_{l=0}^{N}\frac{(i)S_1^{i+k}L^{j+l+1}}{(i+k)(j+l+1)}\right]a_{i,j}k_{k,l} + \left[A_{55}\sum_{i=0}^{M}\sum_{j=1}^{N}\sum_{k=0}^{M}\sum_{l=0}^{N}\frac{(j)S_1^{i+k+1}L^{j+l}}{(i+k+1)(j+l)}\right]a_{i,j}p_{k,l}$$

$$- p_i\sum_{i=0}^{M}\sum_{j=0}^{N}\frac{S_1^{i+1}L^{j+1}}{(i+1)(j+1)}a_{i,j}$$

$$+ \left[\frac{A_{22}}{2R^2}\sum_{i=0}^{M}\sum_{j=0}^{N}\frac{(S_2^{2i+1}-S_1^{2i+1})L^{2j+1}}{(2i+1)(2j+1)} + \frac{A_{44}}{2}\sum_{i=1}^{M}\sum_{j=0}^{N}\frac{(i^2)(S_2^{2i-1}-S_1^{2i-1})L^{2j+1}}{(2i-1)(2j+1)}\right.$$

$$\left. + \frac{A_{55}}{2}\sum_{i=0}^{M}\sum_{j=1}^{N}\frac{(j^2)(S_2^{2i+1}-S_1^{2i+1})L^{2j-1}}{(2i+1)(2j-1)}\right]b_{i,j}^2$$

$$+ \left[\frac{A_{22}}{R^2}\sum_{i=0}^{M}\sum_{j=0}^{N}\sum_{\substack{k=i\\k>i}}^{M}\sum_{\substack{l>j\\l=0}}^{N}\frac{(S_2^{i+k+1}-S_1^{i+k+1})L^{j+l+1}}{(i+k+1)(j+l+1)} + A_{44}\sum_{i=1}^{M}\sum_{j=0}^{N}\sum_{\substack{k=i\\k>i}}^{M}\sum_{\substack{l>j\\l=0}}^{N}\frac{(ik)(S_2^{i+k-1}-S_1^{i+k-1})L^{j+l+1}}{(i+k-1)(j+l+1)}\right.$$

$$\left. + A_{55}\sum_{i=0}^{M}\sum_{j=1}^{N}\sum_{\substack{k=i\\k>i}}^{M}\sum_{\substack{l>j\\l=1}}^{N}\frac{(jl)(S_2^{i+k+1}-S_1^{i+k+1})L^{j+l-1}}{(i+k+1)(j+l-1)}\right]b_{i,j}b_{k,l}$$

$$+ \left[\frac{A_{22}}{R}\sum_{i=0}^{M}\sum_{j=0}^{N}\sum_{k=1}^{M}\sum_{l=0}^{N}\frac{(k)(S_2^{i+k}-S_1^{i+k})L^{j+l+1}}{(i+k)(j+l+1)} - \frac{A_{44}}{R}\sum_{i=1}^{M}\sum_{j=0}^{N}\sum_{k=0}^{M}\sum_{l=0}^{N}\frac{(i)(S_2^{i+k}-S_1^{i+k})L^{j+l+1}}{(i+k)(j+l+1)}\right]b_{i,j}d_{k,l}$$

$$+ \frac{A_{12}}{R}\sum_{i=0}^{M}\sum_{j=0}^{N}\sum_{k=0}^{M}\sum_{l=1}^{N}\frac{(l)(S_2^{i+k+1}-S_1^{i+k+1})L^{j+l}}{(i+k+1)(j+l)}b_{i,j}g_{k,l} + A_{44}\sum_{i=1}^{M}\sum_{j=0}^{N}\sum_{k=0}^{M}\sum_{l=0}^{N}\frac{(i)(S_2^{i+k}-S_1^{i+k})L^{j+l+1}}{(i+k)(j+l+1)}b_{i,j}l_{k,l}$$

$$+ A_{55}\sum_{i=0}^{M}\sum_{j=1}^{N}\sum_{k=0}^{M}\sum_{l=0}^{N}\frac{(j)(S_2^{i+k+1}-S_1^{i+k+1})L^{j+l}}{(i+k+1)(j+l)}b_{i,j}q_{k,l} - p_i\sum_{i=0}^{M}\sum_{j=0}^{N}\frac{(S_2^{i+1}-S_1^{i+1})L^{j+1}}{(i+1)(j+1)}b_{i,j}$$

$$+ \left[\frac{A_{22}}{2}\sum_{i=1}^{M}\sum_{j=0}^{N}\frac{(i^2)S_1^{2i-1}L^{2j+1}}{(2i-1)(2j+1)} + \frac{A_{66}}{2}\sum_{i=0}^{M}\sum_{j=1}^{N}\frac{(j^2)S_1^{2i+1}L^{2j-1}}{(2i+1)(2j-1)}\right]c_{i,j}^2$$

$$+\left[A_{22}\sum_{i=1}^{M}\sum_{j=0}^{N}\sum_{\substack{k=i\\k>i}}^{M}\sum_{\substack{l>j\\l=0}}^{N}\frac{(ik)S_1^{i+k-1}L^{j+l+1}}{(i+k-1)(j+l+1)}+A_{66}\sum_{i=0}^{M}\sum_{j=1}^{N}\sum_{\substack{k=i\\k>i}}^{M}\sum_{\substack{l>j\\l=1}}^{N}\frac{(jl)S_1^{i+k+1}L^{j+l-1}}{(i+k+1)(j+l-1)}\right]c_{i,j}c_{k,l}$$

$$+\left[A_{12}\sum_{i=1}^{M}\sum_{j=0}^{N}\sum_{k=0}^{M}\sum_{l=1}^{N}\frac{(il)S_1^{i+k}L^{j+l}}{(i+k)(j+l)}+A_{66}\sum_{i=0}^{M}\sum_{j=1}^{N}\sum_{k=1}^{M}\sum_{l=0}^{N}\frac{(jk)S_1^{i+k}L^{j+l}}{(i+k)(j+l)}\right]c_{i,j}f_{k,l}$$

$$+\left[\frac{A_{22}}{2}\sum_{i=1}^{M}\sum_{j=0}^{N}\frac{(i^2)(S_2^{2i-1}-S_1^{2i-1})L^{2j+1}}{(2i-1)(2j+1)}+\frac{A_{44}}{2R^2}\sum_{i=0}^{M}\sum_{j=0}^{N}\frac{(S_2^{2i+1}-S_1^{2i+1})L^{2j+1}}{(2i+1)(2j+1)}\right.$$

$$\left.+\frac{A_{66}}{2}\sum_{i=0}^{M}\sum_{j=1}^{N}\frac{(j^2)(S_2^{2i+1}-S_1^{2i+1})L^{2j-1}}{(2i+1)(2j-1)}\right]d_{i,j}^2$$

$$+\left[A_{22}\sum_{i=1}^{M}\sum_{j=0}^{N}\sum_{\substack{k=i\\k>i}}^{M}\sum_{\substack{l>j\\l=0}}^{N}\frac{(ik)(S_2^{i+k-1}-S_1^{i+k-1})L^{j+l+1}}{(i+k-1)(j+l+1)}+\frac{A_{44}}{R^2}\sum_{i=0}^{M}\sum_{j=0}^{N}\sum_{\substack{k=i\\k>i}}^{M}\sum_{\substack{l>j\\l=0}}^{N}\frac{(S_2^{i+k+1}-S_1^{i+k+1})L^{j+l+1}}{(i+k+1)(j+l+1)}\right.$$

$$\left.+A_{66}\sum_{i=0}^{M}\sum_{j=1}^{N}\sum_{\substack{k=i\\k>i}}^{M}\sum_{\substack{l>j\\l=1}}^{N}\frac{(jl)(S_2^{i+k+1}-S_1^{i+k+1})L^{j+l-1}}{(i+k+1)(j+l-1)}\right]d_{i,j}d_{k,l}$$

$$+\left[A_{12}\sum_{i=1}^{M}\sum_{j=0}^{N}\sum_{k=0}^{M}\sum_{l=1}^{N}\frac{(il)(S_2^{i+k}-S_1^{i+k})L^{j+l}}{(i+k)(j+l)}+A_{66}\sum_{i=0}^{M}\sum_{j=1}^{N}\sum_{k=1}^{M}\sum_{l=0}^{N}\frac{(jk)(S_2^{i+k}-S_1^{i+k})L^{j+l}}{(i+k)(j+l)}\right]d_{i,j}g_{k,l}$$

$$-\frac{A_{44}}{R}\sum_{i=0}^{M}\sum_{j=0}^{N}\sum_{k=0}^{M}\sum_{l=0}^{N}\frac{(S_2^{i+k+1}-S_1^{i+k+1})L^{j+l+1}}{(i+k+1)(j+l+1)}d_{i,j}l_{k,l}$$

$$+\left[\frac{A_{11}}{2}\sum_{i=0}^{M}\sum_{j=1}^{N}\frac{(j^2)S_1^{2i+1}L^{2j-1}}{(2i+1)(2j-1)}+\frac{A_{66}}{2}\sum_{i=1}^{M}\sum_{j=0}^{N}\frac{(i^2)S_1^{2i-1}L^{2j+1}}{(2i-1)(2j+1)}\right]f_{i,j}^2$$

$$+\left[A_{11}\sum_{i=0}^{M}\sum_{j=1}^{N}\sum_{\substack{k=i\\k>i}}^{M}\sum_{\substack{l>j\\l=1}}^{N}\frac{(jl)S_1^{i+k+1}L^{j+l-1}}{(i+k+1)(j+l-1)}+A_{66}\sum_{i=1}^{M}\sum_{j=0}^{N}\sum_{\substack{k=i\\k>i}}^{M}\sum_{\substack{l>j\\l=0}}^{N}\frac{(ik)S_1^{i+k-1}L^{j+l+1}}{(i+k-1)(j+l+1)}\right]f_{i,j}f_{k,l}$$

$$+\left[\frac{A_{11}}{2}\sum_{i=0}^{M}\sum_{j=1}^{N}\frac{(j^2)(S_2^{2i+1}-S_1^{2i+1})L^{2j-1}}{(2i+1)(2j-1)}+\frac{A_{66}}{2}\sum_{i=1}^{M}\sum_{j=0}^{N}\frac{(i^2)(S_2^{2i-1}-S_1^{2i-1})L^{2j+1}}{(2i-1)(2j+1)}\right]g_{i,j}^2$$

$$+\left[A_{11}\sum_{i=0}^{M}\sum_{j=1}^{N}\sum_{\substack{k=i\\k>i}}^{M}\sum_{\substack{l>j\\l=1}}^{N}\frac{(lj)(S_2^{i+k+1}-S_1^{i+k+1})L^{j+l-1}}{(i+k+1)(j+l-1)}\right.$$

$$\left.+A_{66}\sum_{i=1}^{M}\sum_{j=0}^{N}\sum_{\substack{k=i\\k>i}}^{M}\sum_{\substack{l>j\\l=0}}^{N}\frac{(ik)(S_2^{i+k-1}-S_1^{i+k-1})L^{j+l+1}}{(i+k-1)(j+l+1)}\right]g_{i,j}g_{k,l}$$

$$+\left[\frac{A_{44}}{2}\sum_{i=0}^{M}\sum_{j=0}^{N}\frac{S_1^{2i+1}L^{2j+1}}{(2i+1)(2j+1)}+\frac{D_{22}}{2}\sum_{i=1}^{M}\sum_{j=0}^{N}\frac{(i^2)S_1^{2i-1}L^{2j+1}}{(2i-1)(2j+1)}+\frac{D_{66}}{2}\sum_{i=0}^{M}\sum_{j=1}^{N}\frac{(j^2)S_1^{2i+1}L^{2j-1}}{(2i+1)(2j-1)}\right]k_{i,j}^2$$

$$+\left[A_{44}\sum_{i=0}^{M}\sum_{j=0}^{N}\sum_{\substack{k=i\\k>i}}^{M}\sum_{\substack{l>j\\l=0}}^{N}\frac{S_1^{i+k+1}L^{j+l+1}}{(i+k+1)(j+l+1)}+D_{22}\sum_{i=1}^{M}\sum_{j=0}^{N}\sum_{\substack{k=i\\k>i}}^{M}\sum_{\substack{l>j\\l=0}}^{N}\frac{(ik)S_1^{i+k-1}L^{j+l+1}}{(i+k-1)(j+l+1)}\right.$$

$$\left.+D_{66}\sum_{i=0}^{M}\sum_{j=1}^{N}\sum_{\substack{k=i\\k>i}}^{M}\sum_{\substack{l>j\\l=1}}^{N}\frac{(jl)S_1^{i+k+1}L^{j+l-1}}{(i+k+1)(j+l-1)}\right]k_{i,j}k_{k,l}$$

$$+\left[D_{12}\sum_{i=1}^{M}\sum_{j=0}^{N}\sum_{k=0}^{M}\sum_{l=1}^{N}\frac{(il)S_1^{i+k}L^{j+l}}{(i+k)(j+l)}+D_{66}\sum_{i=0}^{M}\sum_{j=1}^{N}\sum_{k=1}^{M}\sum_{l=0}^{N}\frac{(jk)S_1^{i+k}L^{j+l}}{(i+k)(j+l)}\right]k_{i,j}p_{k,l}$$

$$+\left[\frac{A_{44}}{2}\sum_{i=0}^{M}\sum_{j=0}^{N}\frac{(S_2^{2i+1}-S_1^{2i+1})L^{2j+1}}{(2i+1)(2j+1)}+\frac{D_{22}}{2}\sum_{i=1}^{M}\sum_{j=0}^{N}\frac{(i^2)(S_2^{2i-1}-S_1^{2i-1})L^{2j+1}}{(2i-1)(2j+1)}\right.$$

$$\left.+\frac{D_{66}}{2}\sum_{i=0}^{M}\sum_{j=1}^{N}\frac{(j^2)(S_2^{2i+1}-S_1^{2i+1})L^{2j-1}}{(2i+1)(2j-1)}\right]l_{i,j}^2$$

$$+\left[A_{44}\sum_{i=0}^{M}\sum_{j=0}^{N}\sum_{\substack{k=i\\k>i}}^{M}\sum_{\substack{l>j\\l=0}}^{N}\frac{(S_2^{i+k+1}-S_1^{i+k+1})L^{j+l+1}}{(i+k+1)(j+l+1)}+D_{22}\sum_{i=1}^{M}\sum_{j=0}^{N}\sum_{\substack{k=i\\k>i}}^{M}\sum_{\substack{l>j\\l=0}}^{N}\frac{(ik)(S_2^{i+k-1}-S_1^{i+k-1})L^{j+l+1}}{(i+k-1)(j+l+1)}\right.$$

$$\left.+D_{66}\sum_{i=0}^{M}\sum_{j=1}^{N}\sum_{\substack{k=i\\k>i}}^{M}\sum_{\substack{l>j\\l=1}}^{N}\frac{(jl)(S_2^{i+k+1}-S_1^{i+k+1})L^{j+l-1}}{(i+k+1)(j+l-1)}\right]l_{i,j}l_{k,l}$$

$$+\left[D_{12}\sum_{i=1}^{M}\sum_{j=0}^{N}\sum_{k=0}^{M}\sum_{l=1}^{N}\frac{(il)(S_2^{i+k}-S_1^{i+k})L^{j+l}}{(i+k)(j+l)}+D_{66}\sum_{i=0}^{M}\sum_{j=1}^{N}\sum_{k=1}^{M}\sum_{l=0}^{N}\frac{(jk)(S_2^{i+k}-S_1^{i+k})L^{j+l}}{(i+k)(j+l)}\right]l_{i,j}q_{k,l}$$

$$+\left[\frac{A_{55}}{2}\sum_{i=0}^{M}\sum_{j=0}^{N}\frac{S_1^{2i+1}L^{2j+1}}{(2i+1)(2j+1)}+\frac{D_{11}}{2}\sum_{i=0}^{M}\sum_{j=1}^{N}\frac{(j^2)S_1^{2i+1}L^{2j-1}}{(2i+1)(2j-1)}+\frac{D_{66}}{2}\sum_{i=1}^{M}\sum_{j=0}^{N}\frac{(i^2)S_1^{2i-1}L^{2j+1}}{(2i-1)(2j+1)}\right]p_{i,j}^2$$

$$+\left[A_{55}\sum_{i=0}^{M}\sum_{j=0}^{N}\sum_{\substack{k=i\\k>i}}^{M}\sum_{\substack{l>j\\l=0}}^{N}\frac{S_1^{i+k+1}L^{j+l+1}}{(i+k+1)(j+l+1)}+D_{11}\sum_{i=0}^{M}\sum_{j=1}^{N}\sum_{\substack{k=i\\k>i}}^{M}\sum_{\substack{l>j\\l=1}}^{N}\frac{(jl)S_1^{i+k+1}L^{j+l-1}}{(i+k+1)(j+l-1)}\right.$$

$$\left.+D_{66}\sum_{i=1}^{M}\sum_{j=0}^{N}\sum_{\substack{k=i\\k>i}}^{M}\sum_{\substack{l>j\\l=0}}^{N}\frac{(ik)S_1^{i+k-1}L^{j+l+1}}{(i+k-1)(j+l+1)}\right]p_{i,j}p_{k,l}$$

$$+\left[\frac{A_{55}}{2}\sum_{i=0}^{M}\sum_{j=0}^{N}\frac{(S_2^{2i+1}-S_1^{2i+1})L^{2j+1}}{(2i+1)(2j+1)}+\frac{D_{11}}{2}\sum_{i=0}^{M}\sum_{j=1}^{N}\frac{(j^2)(S_2^{2i+1}-S_1^{2i+1})L^{2j-1}}{(2i+1)(2j-1)}\right.$$

$$\left.+\frac{D_{66}}{2}\sum_{i=1}^{M}\sum_{j=0}^{N}\frac{(i^2)(S_2^{2i-1}-S_1^{2i-1})L^{2j+1}}{(2i-1)(2j+1)}\right]q_{i,j}^2$$

$$+\left[A_{55}\sum_{i=0}^{M}\sum_{j=0}^{N}\sum_{\substack{k=i\\k>i}}^{M}\sum_{\substack{l>j\\l=0}}^{N}\frac{(S_2^{i+k+1}-S_1^{i+k+1})L^{j+l+1}}{(i+k+1)(j+l+1)}+D_{11}\sum_{i=0}^{M}\sum_{j=1}^{N}\sum_{\substack{k=i\\k>i}}^{M}\sum_{\substack{l>j\\l=1}}^{N}\frac{(jl)(S_2^{i+k+1}-S_1^{i+k+1})L^{j+l-1}}{(i+k+1)(j+l-1)}\right.$$

$$\left.+D_{66}\sum_{i=1}^{M}\sum_{j=0}^{N}\sum_{\substack{k=i\\k>i}}^{M}\sum_{\substack{l>j\\l=0}}^{N}\frac{(ik)(S_2^{i+k-1}-S_1^{i+k-1})L^{j+l+1}}{(i+k-1)(j+l+1)}\right]q_{i,j}q_{k,l} \tag{A.6}$$

References

Anonymous, 1994. IMSL MATH/LIBRARY User's Manual, Version 3.0. Visual Numerics, Inc., Houston, TX.

Anonymous, 1997. ABAQUS/Standard User's Manual, Volumes I–III. Hibbitt, Karlsson, and Sorensen, Inc., Pawtucket.

Arfken, G.G., 1966. Mathematical Methods for Physicists. Academic Press, New York.

Fletcher, R., 1981. Practical Methods of Optimization. In: Constrained Optimization, vol. 2. John Wiley and Sons, Chichester.

Forbes, B., 1999. A thesis on solution methods for 2-D rings with asymmetry. Master's Thesis, University of Delaware, Newark.

Gill, P.E., Murray, W., 1974. Numerical Methods for Constrained Optimization. Academic Press, London.

Goldfarb, D., Idnani, A., 1983. A numerically stable dual method for solving strictly convex quadratic programs. Mathematical Programming 27, 1–33.

Greenberg, M.D., 1998. Advanced Engineering Mathematics, second ed. Prentice Hall, New Jersey.

Ochoa, O.O., Reddy, J.N., 1992. Finite Element Analysis of Composite Laminates. Kluwer Academic Publishers, Dordrecht.

Powell, M.J.D., 1983. ZQPCVX a FORTRAN subroutine for convex quadratic programming. DAMTP Report NA17, Cambridge, England.

Powell, M.J.D., 1985. On the quadratic programming algorithm of Goldfarb and Idnani. Mathematical Programming Study 25, 46–61.

Preissner, E.C., 2002. Analysis of Cylindrical Composite Shells: Examining the Effects of Asymmetric Construction and a Rounded-square Cross-section. Ph.D. Dissertation, University of Delaware, Newark.

Preissner, E.C., Vinson, J.R., 2002a. Application of theorem of minimum potential energy to a complex structure Part I: two-dimensional analysis. International Journal of Solids and Structures, in this issue.

Preissner, E.C., Vinson, J.R., 2002b. Unique bending boundary layer behaviors in a composite non-circular cylindrical shell. Composites Part B: Engineering, accepted for publication.

Soldatos, K.P., Messina, A., 1998. Vibration studies of cross-ply laminated shear deformable circular cylinders on the basis of orthogonal polynomials. Journal of Sound and Vibration 218 (2), 219–243.

Timoshenko, S., Woinowsky-Krieger, S., 1959. Theory of Plates and Shells, second ed. McGraw-Hill, New York.

Vinson, J.R., 1993. The Behavior of Shells Composed of Isotropic and Composite Materials. Kluwer Academic Publishers, Dordrecht.

Vinson, J.R., 1999. The Behavior of Sandwich Structures of Isotropic and Composite Materials. Technomic Publishing, Lancaster.